

UNCLASSIFIED

AD NUMBER

AD239465

LIMITATION CHANGES

TO:

Approved for public release; distribution is unlimited.

FROM:

**Distribution authorized to U.S. Gov't. agencies and their contractors;
Administrative/Operational Use; JUN 1960. Other requests shall be referred to Air Force Arnold Engineering Development Center, Attn: AEDC/IN (STINFO), 251 First Street, Arnold AFB, TN 37389-2305.**

AUTHORITY

AEDC per email dtd 14 Aug 2014 (ltr dtd 14 Sep 2014)

THIS PAGE IS UNCLASSIFIED

AEDC-TR-58-12
(REVISED)



**SOME STUDIES OF THE FLOW PATTERN
AT THE BASE OF MISSILES
WITH ROCKET EXHAUST JETS**

By
B. H. Goethert and L. T. Barnes
ETF, ARO, Inc.

June 1960

cy. 1

**ARNOLD ENGINEERING
DEVELOPMENT CENTER**
AIR RESEARCH AND DEVELOPMENT COMMAND



Additional copies of this report may be obtained from

ASTIA (TISVV)
ARLINGTON HALL STATION
ARLINGTON 12, VIRGINIA

note

Department of Defense contractors must be established for ASTIA services, or have their need-to-know certified by the cognizant military agency of their project or contract.

SOME STUDIES OF THE FLOW PATTERN
AT THE BASE OF MISSILES
WITH ROCKET EXHAUST JETS

By

B. H. Goethert and L. T. Barnes
ETF, ARO, Inc.

This report was originally presented at the Third Technical Symposium on Ballistic Missiles, Los Angeles, California, July 15, 1958, and later published in October 1958 as Confidential and Proprietary.

June 1960

ARO Project No. 101827

Contract No. AF 40(600)-800

CONTENTS

	<u>Page</u>
ABSTRACT	4
NOMENCLATURE	4
INTRODUCTION	5
EXPLORATORY TESTS WITH A SIMPLE COLD FLOW STUDY MODEL	6
SIMILARITY PARAMETERS FOR SIMULATING JET EXHAUSTS	7
STUDIES OF MODEL SIMULATING SOME ATLAS MISSILE CONFIGURATIONS	14
PRESURES AT THE BASE OF THREE-ROCKET MODEL CONFIGURATION	16
DETAIL PROBING OF THE FLOW PATTERN IN THE BASE REGION	18
TURBINE EXHAUST OF ANNULAR SHAPE SURROUNDING THE SUSTAINER ROCKET	19
CONCLUDING REMARKS	20
REFERENCES	21

ILLUSTRATIONS

<u>Figure</u>	<u>Page</u>
1. Launching of an Atlas Intercontinental Ballistic Missile	22
2. Initial 6-in. Cold Flow Study Model	23
3. Smoke Tests with Study Model (smoke probe on vertical centerline)	24
4. Smoke Tests with Study Model (smoke probe at center of model)	25
5. Direction of Flow in the Base of the Study Model	26
6. Schematic of Flow Pattern at Model Base	26
7. Mixing Zone Characteristics	27
8. Schlieren Photographs of Model Nozzles	
a. Sustainer Nozzle, $A/A^* = 11.3$, Chamber Pressure of 150 psia	28
b. Booster Nozzle, $A/A^* = 5.12$, Chamber Pressure of Approximately 150 psia	28

<u>Figure</u>	<u>Page</u>
9. A Test Configuration of a Cold Flow Atlas Model	
a. Top View	29
b. End View	30
10. Smoke Tests with a Special Test Configuration of a Cold Flow Atlas Model without External Flow (smoke velocity is approximately Mach 0.50; note booster turbine exhaust canted overboard and straight sustainer turbine exhaust duct.)	31
11. Effect of an Increase in Velocity of Turbine Exhaust Gases (Special Test Configuration)	32
12. Subsonic Test Chamber.	33
13. Tests of an Atlas Cold Flow Model (Special Test Configuration) in a Subsonic Test Chamber	
a. External Flow Velocity Mach 0.33; Smoke Velocity Mach 1.3	34
b. External Flow Velocity Mach 0.80; Mica Velocity Approximately Mach 1.3	34
c. External Flow Velocity Mach 0.80; Mica Velocity Approximately 0.60	34
14. Location of Base Pressure Instrumentation	35
15. Base Pressure Coefficients for the Atlas Cold Flow Model as a Function of the External Flow Velocity.	36
16. Influence of Rocket Motor Chamber Pressure on the Base Pressure Coefficient.	37
17. Smoke Studies Using a Probe Which Could Be Rotated around Periphery of Sustainer Nozzles	38
18. Studies of Base Flow Patterns Using Small Particles	
a. Path of 1/16-in. Plastic Bead Ejected into Base of Atlas Cold Flow Model	39
b. Paths of Several Styrofoam Particles Ejected into Base of Atlas Cold Flow Model	39
19. Flow Pattern in Base of Atlas Cold Flow Model Based on Tests Using Small Particle Ejection Method	40
20. Cross Section of Annular Sustainer Turbine Exhaust Duct and Sustainer Motor Model Nozzle (Similar to NAA-Rocketdyne Exhausterator Design)	41
21. Tests with an Annular Sustainer Turbine Exhaust Duct at External Flow Velocity of Mach 0.50	42

ABSTRACT

The problem of the recirculation of hot exhaust gases into the engine compartment at the base of a missile has been investigated. Cold flow nozzles were used to simulate the rockets at the base of a missile model, and various tracer techniques were used to visually show the flow pattern at the base. Results are presented for a two-nozzle exploratory model and for various base configurations of the Atlas missile. Similarity parameters for simulating jet exhausts and their application to these investigations are discussed.

NOMENCLATURE

A_B	Area of model base
D	Diameter
M	Mach number
M_a	Mass flow of air
P	Absolute pressure
q	Dynamic pressure, $1/2 \rho V^2$
u	Velocity component in x-direction
v	Velocity component in y-direction
V	Velocity
x, y	Coordinates in intrinsic coordinate system
γ	Ratio of specific heats
Δ	Change in, differential
ϵ	Exchange coefficient
θ	Streamline angle
ρ	Density
σ	Similarity parameter for homogeneous coordinate y/x
ν	Kinematic viscosity

SUBSCRIPTS

j	Jet
s	Static
t	Total
∞	Free-stream

INTRODUCTION

This report gives a brief summary of the studies which are being conducted in the Engine Test Facility of the Arnold Engineering Development Center (AEDC) of the problem of recirculation at the base of ballistic missiles having liquid rocket exhausts.*

An introduction to the problem is afforded by considering some of the effects of base recirculation on a missile such as the Atlas ICBM. A photograph of one of the recent firings of the Atlas is shown in Fig. 1. For this flight the missile was equipped with two booster rockets only. The exhaust of the main rockets can be seen plainly. Also the turbine exhaust, indicated by the cloud to the right of the missile, is clearly visible. Because the exhaust gases of the main rockets and of the turbine are fuel-rich, afterburning can occur when these combustible gases are mixed with atmospheric air. Under certain conditions in flight, as well as during captive firings, the low pressure area at the missile base produced by the external flow action may suck some of the air and some of the exhaust gases backward into the base area and into the engine compartment within the skirt of the missile. If the mixture ratio happens to be suitable and if sufficient stay time is permitted within the skirt region, the combustion gases may ignite, and a burning with resulting high temperatures in the skirt area may occur. Destruction of vital engine components such as fuel lines and control lines may result and, in the case of some actual full-scale tests, may have caused damage or even loss of the missile.

The purpose of the AEDC studies is to investigate in the laboratory the base recirculation problem to determine if possible what parameters affect the sucking of exhaust gases back into the engine compartment and to determine how such dangerous conditions can be avoided.

* These investigations, initiated by the Ballistic Missile Division of the Air Research and Development Command, were conducted in close cooperation with the Ramo-Wooldridge Corporation, particularly with Mr. B. H. Hohmann.

EXPLORATORY TESTS WITH A SIMPLE COLD FLOW STUDY MODEL

In order to become familiar with the problem and to obtain information on suitable testing methods for defining the base recirculation flow, a simple study model was built at AEDC early in 1958. This model (Fig. 2) is not an exact facsimile of an existing ballistic missile. It consists of a two-rocket configuration and an open base area. The two main rocket exhausts are simulated by nozzles which use air as the flow medium. Turbine exhaust flow was simulated by ejecting dense smoke from tubes located at several different positions. By observing the smoke flow, the flow pattern could be visualized, and it could be determined whether or not the smoke was discharging cleanly in the downstream direction away from the missile or whether it was recirculating back into the base region.

These preliminary tests were conducted without external flow to simulate the conditions which occur during captive firings. It should be realized, however, that the exhaust jet pumping action itself generates an external flow which produces a low pressure area in the base region similar to that existing when the missile is in free flight. Some typical pictures of the flow discharge phenomena are presented in Figs. 3 and 4. The smoke can be traced here without difficulty; moreover, it can be seen that when smoke is discharged at short distances from the base (Figs. 3a, 3b, 4a, and 4b) it is sucked back into the base region, a dangerous condition in full-scale applications. On the other hand, when the smoke tube is extended sufficiently downstream (Figs. 3c and 4c), a clean discharge of the smoke from the missile occurs.

By probing the entire base area with these smoke exhaust tubes, it was possible to map the areas in which the flow would proceed downstream out of the base region and the areas in which the flow would circulate back into the base region. These results are shown schematically in Fig. 5. In the region between the rockets, a large area with backflow exists. Only at sufficient distances above and to the outside of both rockets does the flow proceed out of the base region. Shown also in the figure is an area between the two rockets in which the backflow is particularly strong.

The exploratory tests on the initial study model indicated that it is possible to simulate the turbine exhaust gases in the vicinity of operating rocket engines. The results were sufficiently encouraging to justify the application of these techniques to configurations which more closely resembled the full-scale configurations.

SIMILARITY PARAMETERS FOR SIMULATING JET EXHAUSTS

Following the success of preliminary tests with cold flow rockets and smoke exhaust pipes, the next important step was to determine the extent to which the hot rocket exhausts of actual missiles can be simulated by means of cold flow rockets. For laboratory investigations it is more convenient to simulate the rocket exhausts by means of cold airflow than by actually firing rockets, a practice which would necessitate the design and operation of complicated fuel systems and models. For this reason, the main parameters governing the base flow of a missile having rocket exhausts were studied more closely.

The study of the similarity parameters was conducted for supersonic jets exhausting into an external supersonic flow. For all cases, the theoretical relationships became relatively simple. It is expected that the similarity parameters finally obtained will also indicate the conditions existing in subsonic external flow, since pressure gradients of the same type occur in both flows as a function of flow conditions though they differ in the means of propagation.

In Fig. 6, the flow pattern near the base of a model with the rocket in operation is presented schematically. The external flow approaching the rocket base can be simulated to a large extent by a parallel flow with given values (velocity, Mach number, etc.). This flow approaches the base and produces a system of expansion waves which turns the external flow and at the same time reduces the pressure at the boundary of the external flow to the lower pressure of the base region. If the external flow impinges upon the exhaust jet, it must again change its direction, in which case an oblique shock penetrates into the external flow as well as into the rocket exhaust flow. From this general flow pattern it is obvious that two groups of conditions must be met in order to obtain similarity between the exhaust of the actual missile and the cold flow rockets. The first of these is the requirement that similarity be maintained without consideration of the viscosity effects. The second is the requirement that in the mixing region between external flow and the wake, as well as in the mixing region between the rocket exhaust and the wake, similarity in the viscous mixing process, which determines decisively the width and type of the mixing region and the base pressure, should be maintained. In the following paragraphs, the parameters associated with viscous and non-viscous flow will be considered separately.

NON-VISCOUS FLOW REQUIREMENTS

In order to maintain similarity without consideration of the viscous effects, the following conditions (in addition to similarity of geometry, etc.) must be met:

1. External Flow

The static pressure change caused by a change in flow direction for both the full-scale missile and the model must be equal.

2. Exhaust Jet

The static pressure change caused by a change in the flow direction in the jet for the full-scale missile and the model must be equal.

The ratio of the static pressure in the jet at the nozzle exit to the static pressure in the undisturbed external flow for the full-scale missile and the model must be equal.

Static Pressure Change Caused by a Flow Direction Change

A static pressure change caused by a change in the flow direction of the supersonic flow can be presented by the following linearized relationship which should be satisfactory for the accuracy required:

$$\Delta P_s = - \frac{2}{\sqrt{M^2 - 1}} \left(\frac{\rho V^2}{2} \right) \Delta \theta \quad (1)$$

This leads to the final relationship:

$$\frac{\Delta P_s / P_s}{\Delta \theta} = - \frac{\gamma M^2}{\sqrt{M^2 - 1}} \quad (2)$$

In the case of the external flow, the ratio of specific heats (γ) is normally unchanged between the full-scale missile test and the laboratory test. Consequently, the Mach number for the model tests must be equal to the Mach number for the full-scale tests.

However, the ratio of specific heats (γ) of the missile exhaust jet is generally different from the ratio of specific heats for the air which is normally used for cold flow laboratory tests. Consequently, the following relationship between model and full-scale tests must be satisfied:

$$\left(\frac{\gamma M_j^2}{\sqrt{M_j^2 - 1}} \right)_{model} = \left(\frac{\gamma M_j^2}{\sqrt{M_j^2 - 1}} \right)_{full scale} \quad (3)$$

This equation can be met in the case of different specific heat ratios only when the Mach number is adjusted and, therefore, is different for full-scale missile and model exhaust jets. In the case of a full-scale

rocket exhaust nozzle having an exit Mach number of 4.0 and an effective γ of 1.2, it is necessary that the model, operating with a γ of 1.4, have an exit Mach number of 3.53. These two jets would exhibit the same relative static pressure change produced by a change in the direction of flow.

If the Mach number were not adjusted and the model operated at the same Mach number as the full-scale missile, but with a γ of 1.4 instead of 1.2, the static pressure change caused by the same flow angularity change would be larger by the ratio of 1.4/1.2. Whether or not such a deviation from the similarity rules is significant with respect to the main characteristics of the base flow is yet to be investigated.

The static pressure change resulting from the change in flow direction is based on the two-dimensional linear relationship (Eq. 2) when conditions in the immediate vicinity of the shock or expansion waves are considered. The pressure change in the immediate vicinity of the disturbance waves for the base flow also is properly represented by the above linear two-dimensional relationship. However, at larger distances from the waves, deviations occur which tend to produce a pressure change which is smaller than the change represented by Eq.(2).

Exhaust Exit Pressure in Relationship to the Undisturbed Flow Pressure

According to basic compressible flow relationships with a constant γ , the exit pressure at the exhaust of the rocket is related to the chamber pressure by the following:

$$\frac{P_{tj}}{P_{s_j}} = \left[1 + \frac{\gamma - 1}{2} M_j^2 \right]^{\frac{\gamma}{\gamma - 1}} \quad (4)$$

When the exit pressure is expressed in terms of the undisturbed pressure of the flow, P_s , Eq. (4) leads to the following expression:

$$\frac{P_{s_\infty}}{P_{s_j}} = \frac{P_{s_\infty}}{P_{tj}} \left[1 + \frac{\gamma - 1}{2} M_j^2 \right]^{\frac{\gamma}{\gamma - 1}} \quad (5)$$

Since the exit pressure ratio must be the same for both full-scale and model, the following basic condition must then be satisfied:

$$\left\{ \frac{P_{s_\infty}}{P_{tj}} \left[1 + \frac{\gamma - 1}{2} M_j^2 \right]^{\frac{\gamma}{\gamma - 1}} \right\}_{model} = \left\{ \frac{P_{s_\infty}}{P_{tj}} \left[1 + \frac{\gamma - 1}{2} M_j^2 \right]^{\frac{\gamma}{\gamma - 1}} \right\}_{full scale} \quad (6)$$

It can be seen from this equation that when the same γ and exit Mach number are used for both the full-scale and the model, the model must be operated at the same ratio of chamber pressure to exhaust pressure as is the full-scale rocket. On the other hand, if the γ is changed from the full-scale value of 1.2 to the cold flow value of 1.4 and the Mach number is changed from 4.0 to 3.53, similarity can be maintained only if the model chamber pressure is reduced. In the case of a full-scale rocket motor having an operating chamber pressure of 600 psia, the simulated chamber pressure of the model must then be lowered to 155 psia.

VISCOUS FLOW REQUIREMENTS

The viscosity effects are of importance only in the mixing region between the external flow and the exhaust jet with wake behind the base of the model. The problem therefore reduces to the determination of similarity parameters for the mixing between an essentially parallel flow and the wake which, for our purposes, can be assumed to have a negligibly small velocity in comparison with the higher velocities of both the external flow and the exhaust jet.

Incompressible Flow

The mixing process can be shown to be governed by the equation of motion which, put in a simplified form for the case of incompressible flow at constant pressure, reads:

$$u \frac{\partial u}{\partial x} + v \frac{\partial u}{\partial y} = \epsilon \frac{\partial^2 u}{\partial y^2} \quad (7)$$

where ϵ represents the kinematic viscosity, v , in laminar flow and the apparent kinematic viscosity in turbulent flow. It is assumed that for the case under consideration, the mixing between a free jet and a wake will follow a turbulent pattern.

Many investigators have conducted studies (based on Prandtl's mixing length theory) of the problem of turbulent mixing. In a modification of his original theory, Prandtl formulated ϵ as an exchange coefficient which, in our notation, can be written:

$$\epsilon = K_1 C x v_\infty \quad (8)$$

In this equation, C determines an experimental constant which characterizes the spread of the mixing zone as a function of the distance, x . K_1 also is a constant which must be determined empirically. Goertler (Ref. 1) introduced Prandtl's exchange coefficient theory into

the equations for continuity and momentum and arrived at the following velocity distribution for the mixing zone:

$$\frac{V}{V_\infty} = \frac{1}{2} \left[1 + \operatorname{erf} \left(\sigma \frac{y}{x} \right) \right] \quad (9)$$

where the error function is defined as:

$$\operatorname{erf} = \frac{\sigma \frac{y}{x}}{\sqrt{\pi}} \int_0^{\frac{y}{x}} e^{-z^2} dz$$

and $\sigma = \frac{1}{2 \sqrt{K_1 C}}$, another constant to be determined. Numerous experiments have shown that in incompressible flow, this distribution function of Goertler's agrees with experimental data when σ is assumed to have values between 12 and 13 (see Ref. 2).

Jet Mixing in Compressible Flow

A number of theoretical studies have been conducted to determine the mixing characteristics of a supersonic jet discharging into a medium at rest for the case of constant temperature and equal gases. It was shown (Ref. 3) that basically Eq. (9) holds true except that σ now becomes a function of the Mach number. Experimental results of several authors show that an approximate value of σ can be obtained with the following equation (Ref. 3):

$$\sigma = 12 + 2.58M \quad (10)$$

If this equation is assumed to be satisfactory it becomes possible to determine the velocity profile in a mixing region for all cases of compressible flow for which the assumptions made above hold true.

It is obvious that the assumptions made above for compressible flow mixing are not satisfied in the case of actual hot exhaust jets since the temperature of the exhaust gas and the surrounding medium, as well as the properties of the two gases, are different. Unfortunately no precise theories are available to predict mixing characteristics accurately in the case of large temperature differences or large differences in the characteristics of the two gases involved. However, first order calculations have been made by Abramovich determining the effect of temperature differences between the exhaust jet and the surrounding medium (Ref. 4) and by S. I. Pai on the influence of various gas properties (Ref. 5). Both investigations indicate that even the first order effects are small. In spite of the different temperatures and the different gas properties involved, the velocity profile in the mixing region is changed only to a very small extent. Moreover, the temperature distribution, as well as the density distributions, follows a law

similar to that of the velocity distribution. Consequently, the density distribution in the mixing region between a jet and a medium at rest where each has a different temperature and different gas characteristics may be approximated by the following equation:

$$\rho = \frac{\rho_j + \rho_\infty}{2} \left[1 + \frac{\rho_j - \rho_\infty}{\rho_j + \rho_\infty} \cdot \operatorname{erf} \left(\sigma \frac{y}{x} \right) \right] \quad (11)$$

(σ to be determined from Eq. 10)

Similarity Parameters for the Influence of Viscosity

With the aid of the relationships stated above for the velocity and density profiles in the mixing region, it is now possible to arrive at specific similarity parameters which must be maintained for jet simulation and to determine the pumping characteristics of the exhaust jet.

Jet Boundary - In the mixing region, parts of the exhaust jet are being decelerated while parts of the surrounding medium are being accelerated because of the viscous effect. Consequently, the entire flow in the mixing region consists of a mass which is larger than the mass of the original jet. It is now possible to determine the coordinate y_j (Fig. 7), which defines the streamline below which the mass flow is equal to the mass flow of the exhaust jet. The flow beyond this streamline represents the additional flow resulting from the pumping action of the exhaust jet on the surrounding medium. The coordinate of this dividing streamline can also be interpreted as a displacement thickness which replaces the actual velocity profile by a distribution having constant velocity. The continuity equation can be utilized to define this value.

$$\int_0^{y_j} \frac{u}{u_j} \cdot \frac{\rho}{\rho_j} dy = \int_{-\infty}^0 \left(1 - \frac{u}{u_j} \cdot \frac{\rho}{\rho_j} \right) dy \quad (12)$$

The jet boundary coordinate y_j can be determined from this equation since the velocity and density profile terms occurring under the integral are known.

Excess Pumping Mass - The entrained mass which is put in motion by a circular exhaust jet can be expressed by the following equation:

$$M_a = \pi D_j \int_{y_j}^{\infty} u \rho dy = V_j \rho_\infty A_B \quad (13)$$

This integral must be extended from the jet boundary coordinate y_j to infinity. The excess pumping mass can be made non-dimensional by means of the velocity and density of the undisturbed flow and with the area of the base A_B . Thus, in non-dimensional form, the excess pumping mass parameter assumes the following form:

$$\frac{\Delta V_j}{V_\infty} = \frac{u_j}{u_\infty} \cdot \frac{\rho_j}{\rho_\infty} \frac{\pi D_j^2}{A_B} \int_{y_j}^{\infty} \frac{u}{u_j} \frac{\rho}{\rho_j} \frac{dy}{D_j}$$

The integral can be determined from the known velocity and density distributions.

Total Pressure at the Jet Boundary Streamline - The excess pumping mass determined previously consists of a mixture of the exhaust gas and the surrounding air. In order to provide the same exhaust discharge conditions for this excess pumping mass, the total pressure head which is available at the dividing streamline of the jet should be determined and placed in relation to the dynamic pressure of the undisturbed flow. These considerations lead finally to the similarity parameter

$$\frac{P_t(y_j)}{q_\infty} = \frac{\rho(y_j) [u(y_j)]^2}{\gamma P_\infty M_\infty^2}$$

In order to maintain similarity between the full-scale process and the model test, it is necessary to simulate these two main parameters, the excess pumping mass parameter and the jet boundary streamline head. The goal of future investigations in the laboratory will be the determination of their separate influences.

Effect of Changes in Simulated Chamber Pressures - It is of interest to determine to what extent the excess pumping mass parameter changes when the chamber pressure is changed for the case of the cold flow rocket. The application of the criteria for the excess pumping mass (Eq. (13)) shows that the chamber pressure for a cold flow rocket nozzle operating at Mach 4.0 can be changed by a factor of 2 (i.e., an increase from 250 psi to 500 psi) while the pumping characteristic parameter changes by no more than approximately 10 percent. The results seem to indicate that the pumping effect of the base jet is only affected slightly by the chamber pressure. Consequently, it may be concluded that the chamber pressure is not a sensitive term in the simulation problem. Results obtained with a cold flow model for which the influence of chamber pressure has been checked experimentally will be discussed later. These experimental results and the theoretical prediction given above are in good agreement.

Separation of Nozzle Flow at Reduced Chamber Pressures - In the preceding calculations, it has been shown that the chamber pressure for cold flow model rockets must be reduced considerably in order to simulate the conditions occurring in full-scale hot jet tests. In many cases, the flow of the hot rockets expands to pressures within the rocket nozzle which are lower than those of the surrounding medium. It is therefore necessary to investigate whether the flow in the model tests fills the exit nozzle in the same manner as the flow in full-scale rocket tests or whether the flow separates. The danger of separation in model tests is considerably increased because the Reynolds number for these tests is generally smaller than that for full-scale tests.

In order to make sure that the nozzle flow for the cold flow experiments behaves in the same way as in full-scale operation, preliminary investigations were made using a schlieren system to determine the critical pressure for flow separation. Two nozzles were investigated; one having an expansion ratio of 11.3 and another having an expansion ratio of 5.12. The nozzles simulate approximately the rocket nozzles of the sustainer and booster rocket motors of the Atlas missile. Some typical schlieren photographs are shown in Fig. 8. It was determined that in neither case did the flow separate at chamber pressures above 100 psi, proof that the flow at the chamber pressure under consideration did not separate but filled the nozzle in the same manner as in the full-scale missile.

STUDIES OF MODEL SIMULATING SOME ATLAS MISSILE CONFIGURATIONS

Models of some Atlas missile base configurations were built, and further investigations of the base recirculation problem were undertaken. A model which has a scale factor of 1:20 is shown in Figs. 9a and 9b. The cold flow rockets were dimensioned in such a way that they simulate approximately the parameters discussed previously. The turbine exhaust ducts were formed according to a special test configuration and were operated with smoke or other light tracer material such as mica in order to provide a means of visualizing the flow pattern. The sustainer turbine exhaust duct was located in the vicinity of the sustainer rocket, and the single common booster-turbine exhaust duct was usually canted sidewise so that the gases were discharged directly into the free-stream flow.

EXPERIMENTS WITHOUT EXTERNAL FLOW

Numerous tests were conducted with the 1/20th-scale model to simulate the conditions during a captive firing, that is, without external flow velocities. Figure 10 is a typical picture of the pattern of the turbine exhaust flows and shows some of the results obtained with a tentative test configuration of the turbine exhaust ducts. It is obvious from these studies that the canted turbine exhaust duct for the booster rockets discharges the smoke cleanly downstream. In the case of the sustainer turbine exhaust duct, however, it is evident that a part of the exhaust products is recirculating back into the base region and creating dangerous conditions. It must be concluded, therefore, that this particular configuration of the sustainer-turbine exhaust (Fig. 10) represents a possible hazard to full-scale operation of the missile.

In the above tests (Fig. 10), the exhaust velocity of both the booster and the selected sustainer turbine exhaust ducts was approximately Mach 0.5. The next step was to determine to what extent the undesirable backflow could be reduced or prevented by increasing the velocity of the sustainer turbine exhaust. It was hoped that by increasing the momentum, the gases would be capable of penetrating into high pressure regions downstream of the base without being sucked back into the base region.

Tests were conducted in which the velocity of the selected sustainer exhaust test configuration was varied from Mach 0.4 to 1.4. Some typical pictures of the smoke flow are presented in Fig. 11. At a Mach number of 0.4, a strong backflow of the exhaust gases existed. This backflow was gradually reduced and nearly disappeared at Mach numbers on the order of 0.8 to 1.0; at supersonic Mach numbers no indication of backflow or recirculation was found. It was concluded from these tests that it is possible to prevent recirculation in the case of captive firings (external velocity zero) when the velocity of the turbine exhaust gases of the sustainer engine can be increased into the supersonic range.

EXPERIMENTS WITH SUBSONIC EXTERNAL FLOW

In order to extend the test operating range into the region of actual missile flight, the construction of subsonic as well as supersonic test chambers in which the 1/20th-scale Atlas cold flow model can be examined under external flow conditions was planned. The subsonic test chamber, which has been completed and placed in operation, is shown in Fig. 12. The tests in this chamber were conducted in the same manner and with the identical model used during the tests made without external flow. The same methods of making flow visible were also used, although powdered mica was employed to a greater extent than smoke. Typical pictures of operation of the same experimental sustainer

turbine exhaust duct configuration, as used before, but with the model installed in the subsonic chamber are shown in Figs. 13a and 13b. These tests were conducted with an external flow velocity of Mach 0.33 and 0.80 and with the sustainer turbine exhaust duct discharge at a velocity of approximately Mach 1.3. Even at this relatively high discharge Mach number, a strong recirculation occurred. This is in contrast to the case of the simulated captive firings during which recirculation was not apparent when the sustainer turbine gases were exhausted at supersonic velocities. However, the canted booster turbine exhaust duct (Fig. 13c), operated only at Mach 0.5, continued to discharge the exhaust gases cleanly downstream as in the case of the captive firings.

Obviously the increased intensity of the low pressure region at the base of a missile with external flow causes the flow recirculation to be more severe than in the case of captive firings. Even though a given turbine exhaust configuration successfully and safely discharges the exhaust gases during a captive firing, severe backflow of exhaust gases into the engine compartment may still occur as a result of the more severe conditions with external flow.

Investigations have been in progress at AEDC for some time to determine the effectiveness of proposed modifications to the turbine exhaust systems. At the time of these tests, the status of the problem was to select a suitable turbine exhaust. The sustainer exhaust shown in the previous figure was not a final design configuration. The efforts have been directed particularly toward ventilating the missile base region and toward obtaining quantitative data on flow direction and distribution in the base region. In addition to the smoke method of flow visualization, more detailed tracer methods have been developed which consist of ejecting small particles into the flow to determine the individual streamline pattern in the region of interest.

PRESSURES AT THE BASE OF THREE-ROCKET MODEL CONFIGURATION

BASE PRESSURE MEASUREMENTS

The 1/20th-scale Atlas missile model discussed previously was equipped with several static pressure pickups to obtain representative static pressure data. In Fig. 14, for instance, the location of three static pressure orifices is shown. Two of them were located at the bulkhead at the base of the engine compartment; the third was located so as to measure the static pressure in the base exit plane between the two nozzles of the operating rockets.

Some results of the static pressure measurements are presented in Fig. 15. With external flows up to Mach 0.6, the base pressure

coefficient without rocket flow was nearly constant and had a magnitude which matched satisfactorily the base pressure coefficient determined in other experiments with similar models. With the cold flow rockets operating, the base pressure was considerably decreased. At low external-flow velocities the effect of the exhaust jets on the magnitude of the base-pressure coefficient is considerably larger than the effects of the external flow; at velocities of external flow of Mach 0.6, the effects were approximately equal. When these data are translated into actual pressure differences (ΔP) by multiplying by the value of the dynamic pressure of the undisturbed flow, the absolute value of ΔP increases with increasing Mach number so that the tendency to suck exhaust gases back into the base region is increased with increasing Mach number. This result of the static pressure measurements seems to bear out the results obtained with the smoke studies which indicated that with external flow the conditions are more severe than in the case of captive firings.

Additional experiments with the emphasis on the determination of the static pressure field, not only in the exit plane of the missile, but also downstream, are being conducted. The results will indicate the static pressure rise which the exhaust gases must overcome in order to discharge cleanly in the downstream direction.

INFLUENCE OF CHAMBER PRESSURE ON BASE PRESSURE

The results of the static pressure measurements of the Atlas missile model discussed in the previous paragraph were obtained using a constant rocket motor chamber pressure which simulates the conditions necessary to maintain the similarity between the full-scale missile and model. In order to check the sensitivity of the current setting of the chamber pressure, some of the previous experiments were repeated with the chamber pressure varying over wide ranges. In Fig. 16, the static pressure at the base of the missile is presented for an external flow velocity of Mach 0.5 and a booster rocket chamber pressure ranging from 140 to 500 psi. For these experiments, the sustainer rocket chamber pressure was kept constant. It is evident that the influence of the chamber pressure magnitude within the limits noted is negligible. This is in agreement with the theoretical error prediction described previously, that the changes in chamber pressure will have only slight effect on the pumping effect of a jet with given nozzle geometry. It also indicates further that it may be possible to simulate satisfactorily the hot flow conditions with the cold flow conditions of the model tests.

The chamber pressures shown in Fig. 16 cover a range in which, according to the preliminary schlieren investigations, the flow is clearly attached to the nozzle walls so that no disturbing secondary effects due to flow separation occur.

DETAIL PROBING OF THE FLOW PATTERN IN THE BASE REGION

As indicated before, several means were employed to determine the flow pattern and vortex system in the base region. The various vortices formed in this region were detected by the emission of smoke from moving probes or by the ejection into the flow of small particles which are supposed to float along with the streamlines of the main flow.

ROTATING SMOKE PROBE EXPERIMENTS

A smoke probe emitting smoke at a very low velocity was supported in such a way that it could be rotated around the sustainer rocket nozzle. In this way the region in which the flow proceeds downstream or upstream into the base region was indicated. The probe arrangement and some results obtained are presented in Fig. 17.

It is evident from these figures that along the engine circumference of the sustainer rocket exhaust nozzle, the flow does not discharge downstream at any point. Between the sustainer and booster rocket, a strong backflow upstream into the engine compartment exists. From the top position on the sustainer rocket nozzle, the flow follows a tangential path along the circumference of the sustainer rocket exit until it meets the strong back flow region between the rockets and proceeds from there back into the engine compartment. These tests indicate that the interference between two exhaust jets is a predominant factor in governing the base flow pattern and must be considered the most critical portion of the entire flow problem.

SMALL PARTICLE EJECTION METHOD

One important method of obtaining the flow pattern of the base region was the ejection of small particles in the base region. Efforts were made to obtain and use particles which would have a large drag comparable to their mass so that they would follow the streamlines of the flow as closely as possible.

In one case, very small, light dylite beads were individually ejected into the base region at zero velocity, and their paths were recorded by means of high speed cameras. Some results of this type of experiment are shown in Fig. 18a which is a composite picture of one particle superimposed on one frame of the film.

In the second method, a large number of small styrofoam particles were emitted into the base region at a very low velocity, and their paths were again recorded using high speed photographic methods. Some results of this type of experiment are shown in Fig. 18b which also is a composite picture.

As in previous experiments the small particle ejection method showed that the flow proceeds backward into the base region between the two operating rockets, then proceeds to the outer extremities of the base region. A large number of experiments of this type have been conducted, and an effort has been made to determine the vortex pattern which exists in the base region. The methods used for these tests are still being perfected.

A typical streamline picture that has been obtained for the flow which occurs within the skirt region (Fig. 19) indicates that in the interior area surrounding the sustainer rocket and between the rockets, a strong backflow exists. Only in the narrow region along the edges of the missile skirt does the flow proceed downstream in the desired direction. The complex vortex system within the base is clearly evident. The investigation is now being extended to define the vortex flow system external to the base.

TURBINE EXHAUST OF ANNULAR SHAPE SURROUNDING THE SUSTAINER ROCKET

In the preceding experiments, it was determined that the flow proceeds inward into the base region at or very close to the exit of the sustainer rocket. This was somewhat surprising since a major part of the difficulties is caused by the fact that the jet accelerates and mixes with the wake flow and, therefore, must entrain some of the surrounding air in the direction of the jet.

The experiments, however, seem to indicate that the region of entrainment is extremely thin. This is in line with the mixing theory discussed before which also indicates that with increasing external flow velocity the value of σ increases (Eq. 10), resulting in a decrease of the mixing region. It was believed during the initial phase of the test program that, because of the entrainment action of the main jet, it would be possible to discharge the mixing region gases cleanly downstream. An annular exhaust duct (Fig. 20), similar to the NAA-Rocketdyne exhausterator design, which would guide the turbine exhaust gases into a narrow annular area and bring them in close contact with the main rocket exhaust jet was therefore devised. The suitability of this configuration as a satisfactory sustainer turbine

exhaust was investigated experimentally by emitting fine mica powder from the annular duct. Typical pictures taken with an external flow velocity of Mach 0.3 are shown in Fig. 21. Figure 21a shows the results obtained at the relatively low exhaust pressure of 20 psia; the results shown in Fig. 21b were obtained at an exhaust pressure of 51 psia.

The photographs show clearly that a strong recirculation of the turbine exhaust flow exists and that, consequently, such solutions of the sustainer rocket turbine exhaust problem cannot be assumed to be completely trouble-free. This result is not surprising in view of the mixing region theories presented previously. It is obvious that while it is mixing with the surrounding air, a part of the external boundary flow, including some of the main rocket exhaust, will be slowed down to such low values that the dynamic head will not be large enough to overcome the static pressure drop in the base region. Therefore, even parts of the main rocket exhaust flow have a tendency to flow back into the base region. When the turbine exhaust gases with their smaller dynamic head and much greater content of unburned fuel are added to the boundary region of the main rocket exhaust, the danger of recirculation difficulties becomes more serious. The danger of fire, however, depends upon the quantity of gases recirculated, the presence of a suitable mixture ratio, and sufficient stay time in the engine compartment.

CONCLUDING REMARKS

The preceding excerpts from various phases of studies at AEDC on the base recirculation problem show that attempts are being made by several methods to define the flow pattern at the base of missiles and to determine configurations which are safe for full-scale turbine exhaust application. With quantitative measurements, strongly supported by flow visualization methods, a fuller understanding of the parameters governing the flow pattern should be attained.

In all the described experiments conducted at AEDC, cold flow rockets have been used to simulate the actual exhaust pattern of the full-scale missiles. A 1/10th-scale model of the Atlas missile having three hot burning rockets is under construction and will be subjected to a similar type of testing. By comparing these data, it will be possible to determine the limits of the reliability of simulating hot exhaust flow problems with cold jets in laboratory testing.

REFERENCES

1. Görtler, H. "Berechnung Von Aufgaben der freier Turbulenz auf Grund eines neuen Näherungsansatzes." Z.A.M.M., Vol. 22, 1942. (German)
2. Reichardt, H. VDI Research Paper No. 4141. (German)
3. Korst, H. H., Page, R. H., and Childs, M. E. "Compressible Two-Dimensional Jet Mixing at Constant Pressure." Mechanical Engineering Department, Engineering Experiment Station, University of Illinois. ME Technical Note 392-2, April 1954.
4. Abramovich, G. N. "The Theory of a Free Jet of a Compressible Gas." NACA TM 1058, 1944.
5. Pai, S. I. Fluid Dynamics of Jets. D. Van Nostrand, New York, 1954.



Courtesy Convair Division,
General Dynamics Corporation

**Fig. 1 Launching of an Atlas Intercontinental
Ballistic Missile**

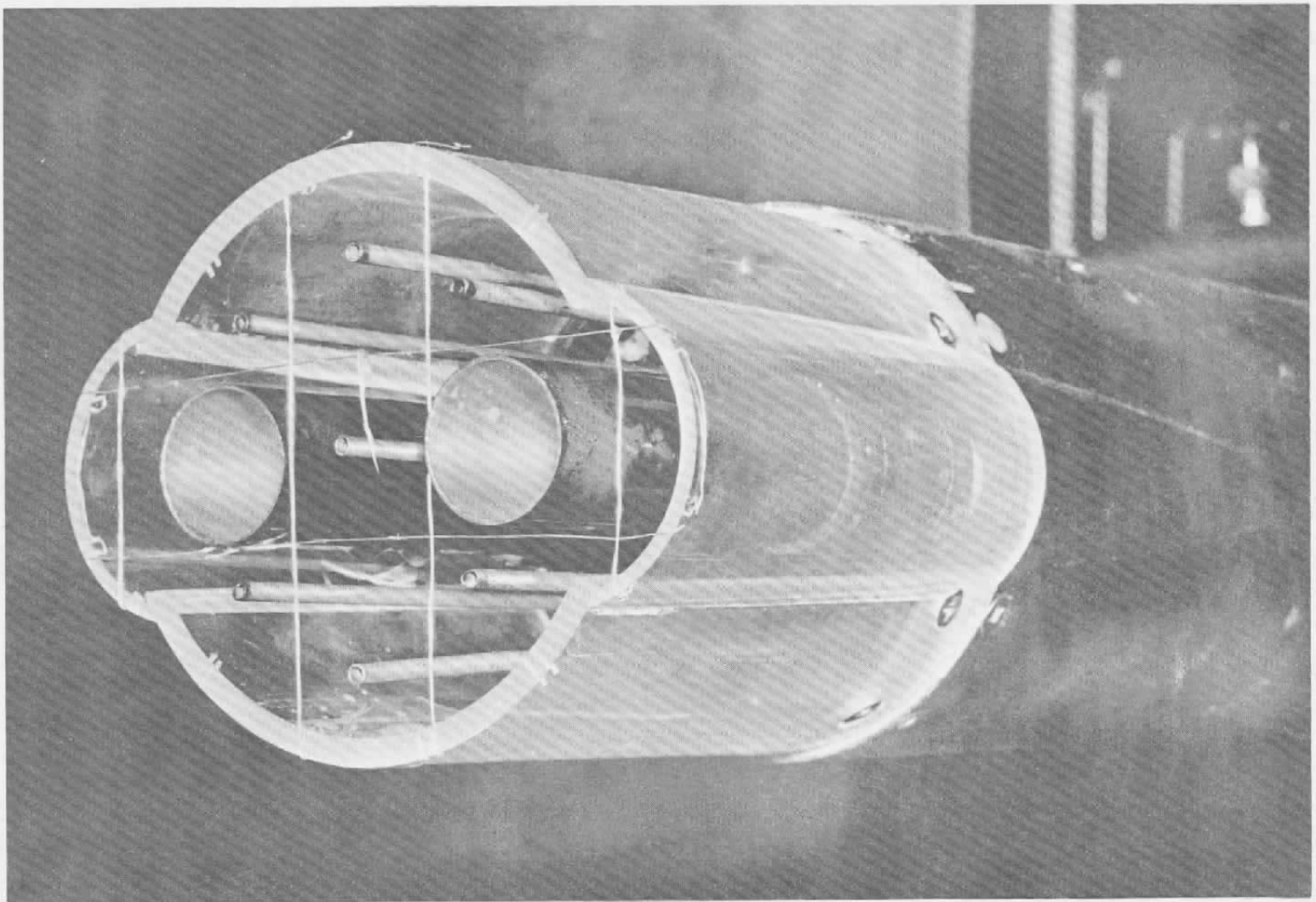


Fig. 2 Initial 6-in. Cold Flow Study Model

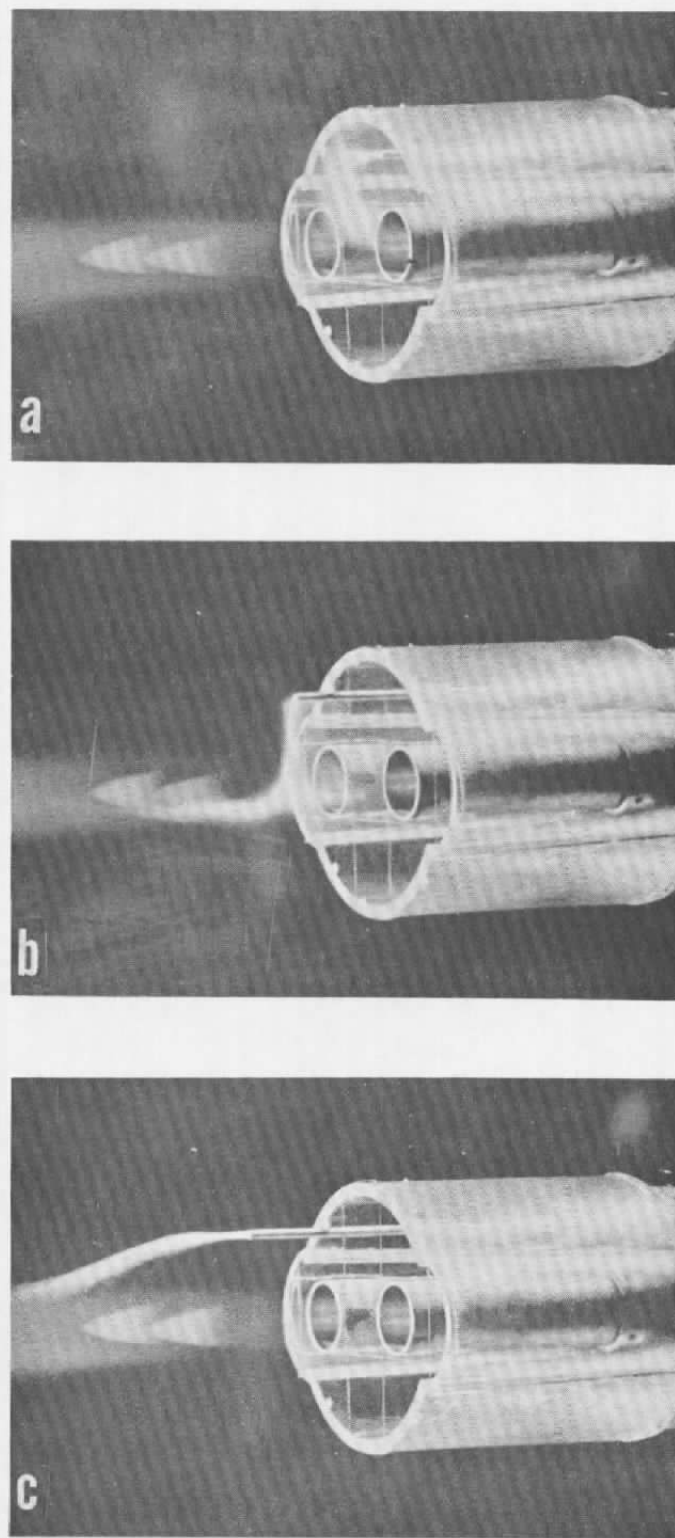


Fig. 3. Smoke Tests with Study Model (smoke probe on vertical centerline)

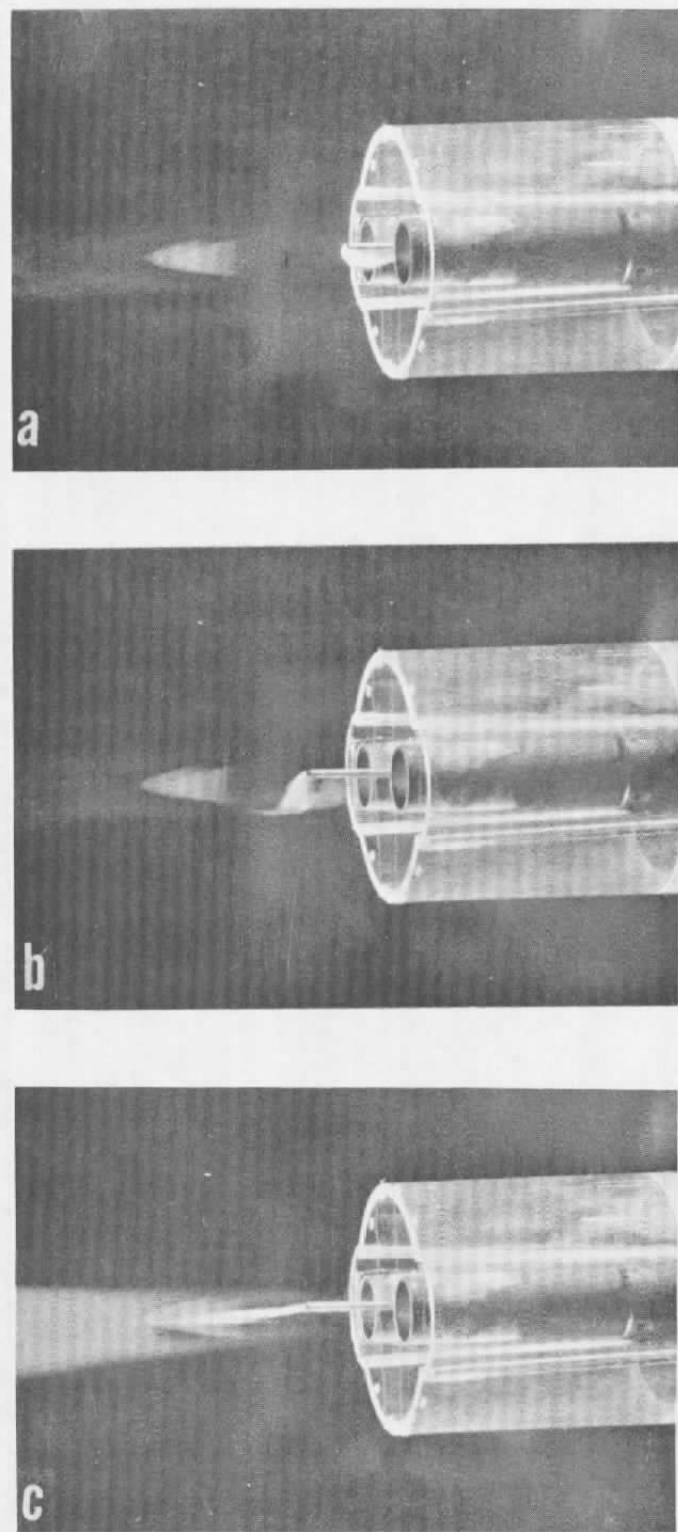


Fig. 4. Smoke Tests with Study Model (smoke probe at center of model)

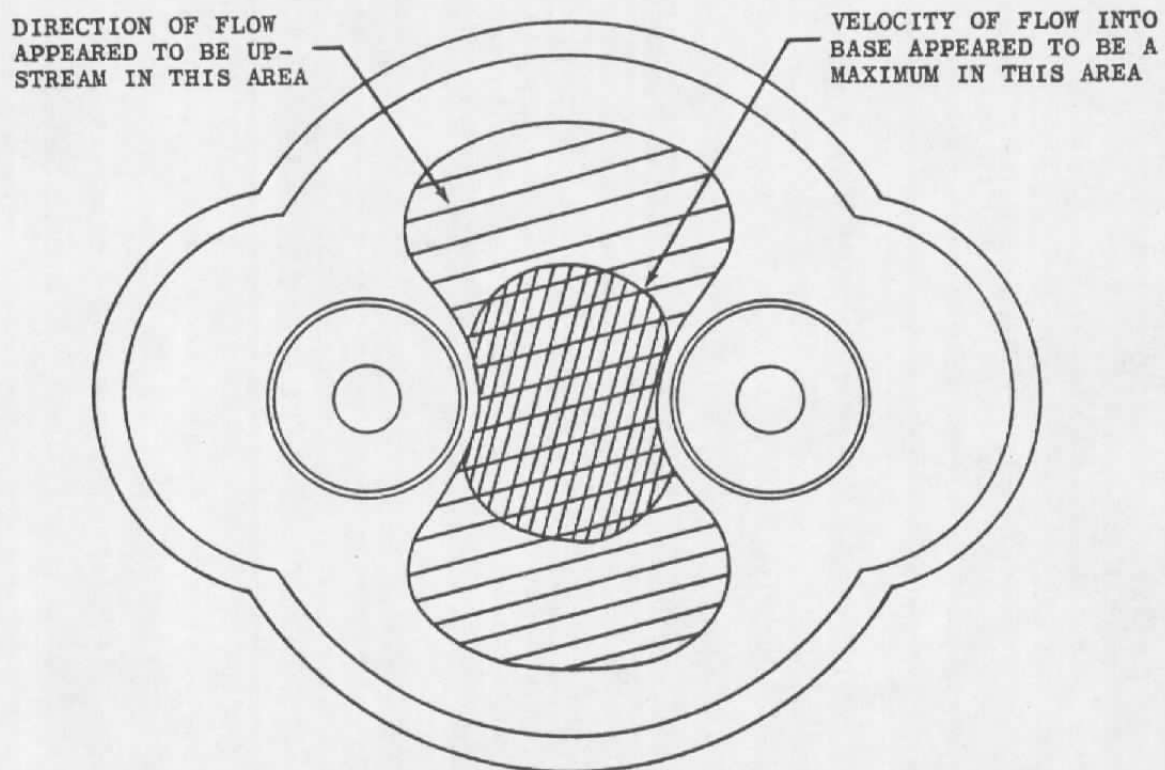


Fig. 5. Direction of Flow in the Base of the Study Model

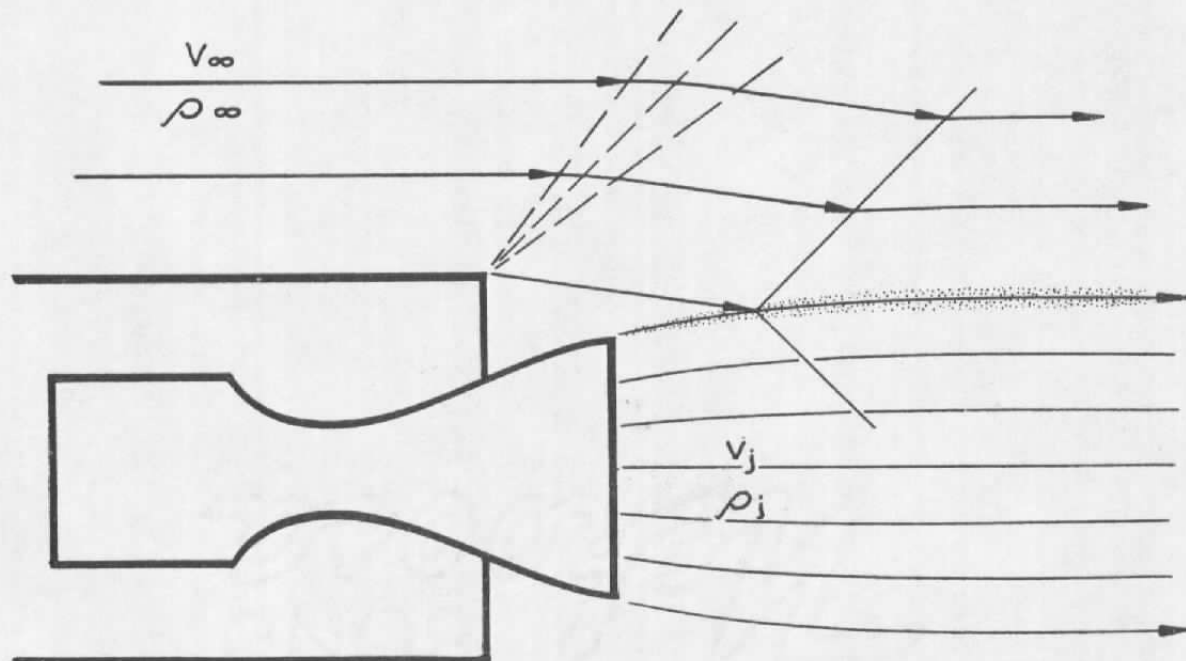
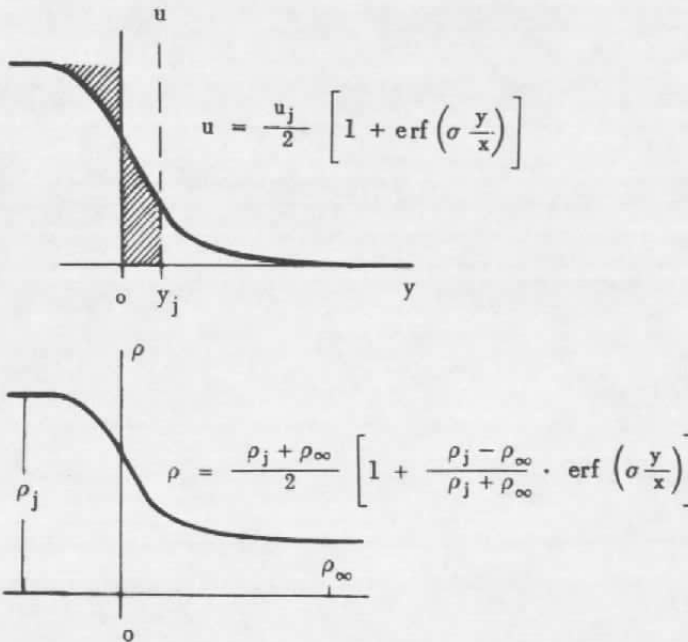
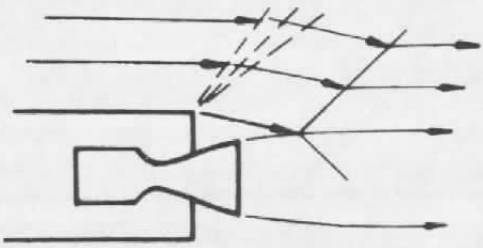


Fig. 6. Schematic of Flow Pattern at Model Base



JET BOUNDARY

$$\int_{-\infty}^{y_j} u \cdot \rho \cdot dy = \int_{-\infty}^0 u_j \cdot \rho_j \cdot dy$$

$$\int_0^{y_j} \frac{u}{u_j} \cdot \frac{\rho}{\rho_j} \cdot dy = \int_{-\infty}^0 \left(1 - \frac{u}{u_j} \cdot \frac{\rho}{\rho_j} \right) dy$$

EXCESS PUMPING MASS

$$M_a = \pi \cdot D_j \int_{y_j}^{\infty} u \cdot \rho \cdot dy = V_j \rho \cdot \rho_\infty \cdot A_B$$

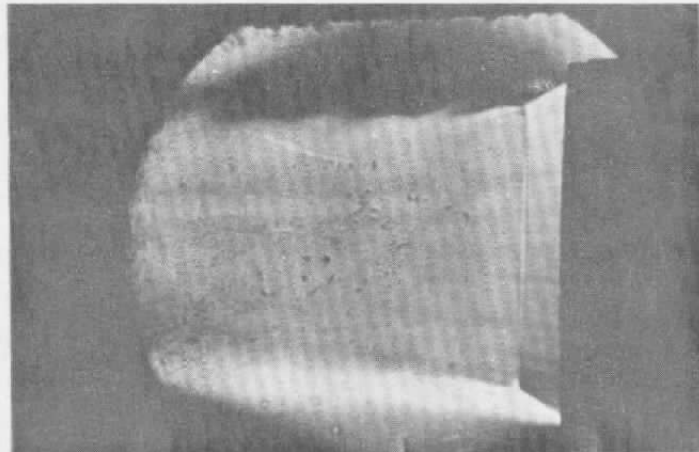
$$\frac{V_{jP}}{V_\infty} = \frac{\pi \cdot D_j}{A_B} \cdot \frac{u_j}{u_\infty} \cdot \frac{\rho_j}{\rho_\infty} \int_{y_j}^{\infty} \frac{u}{u_j} \cdot \frac{\rho}{\rho_j} dy$$

JET BOUNDARY STREAMLINE HEAD

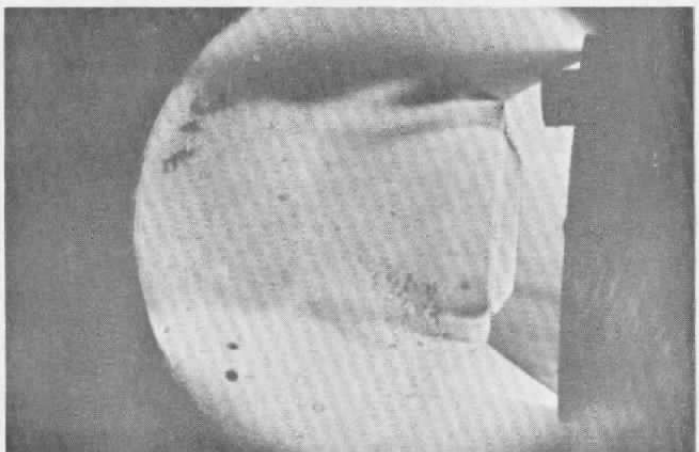
$$P_t(y_j) = \frac{1}{2} \cdot \rho(y_j) \cdot [u(y_j)]^2$$

$$\frac{P_t(y_j)}{q_\infty} = \frac{\rho(y_j) \cdot [u(y_j)]^2}{\gamma \cdot P_\infty \cdot M_\infty^2}$$

Fig. 7. Mixing Zone Characteristics

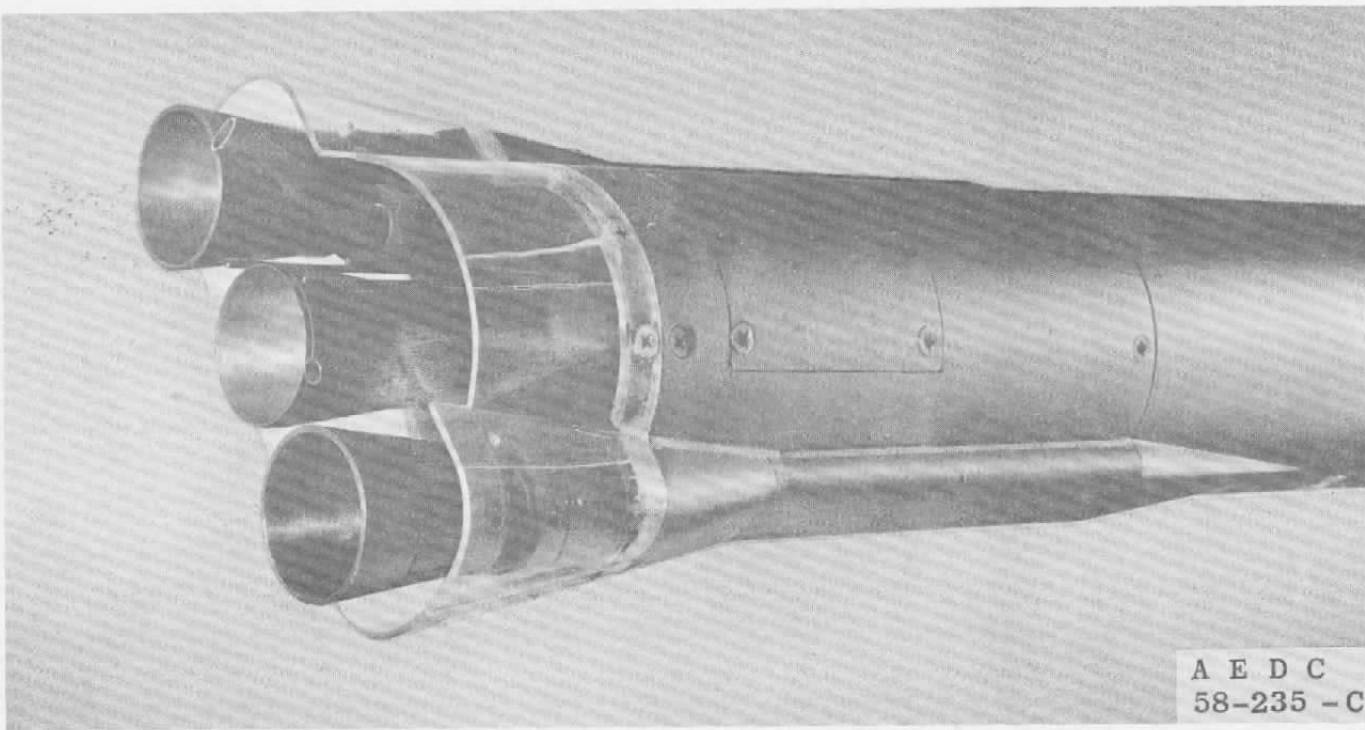


a. Sustainer Nozzle, $A/A^* = 11.3$, Chamber Pressure of 150 psia



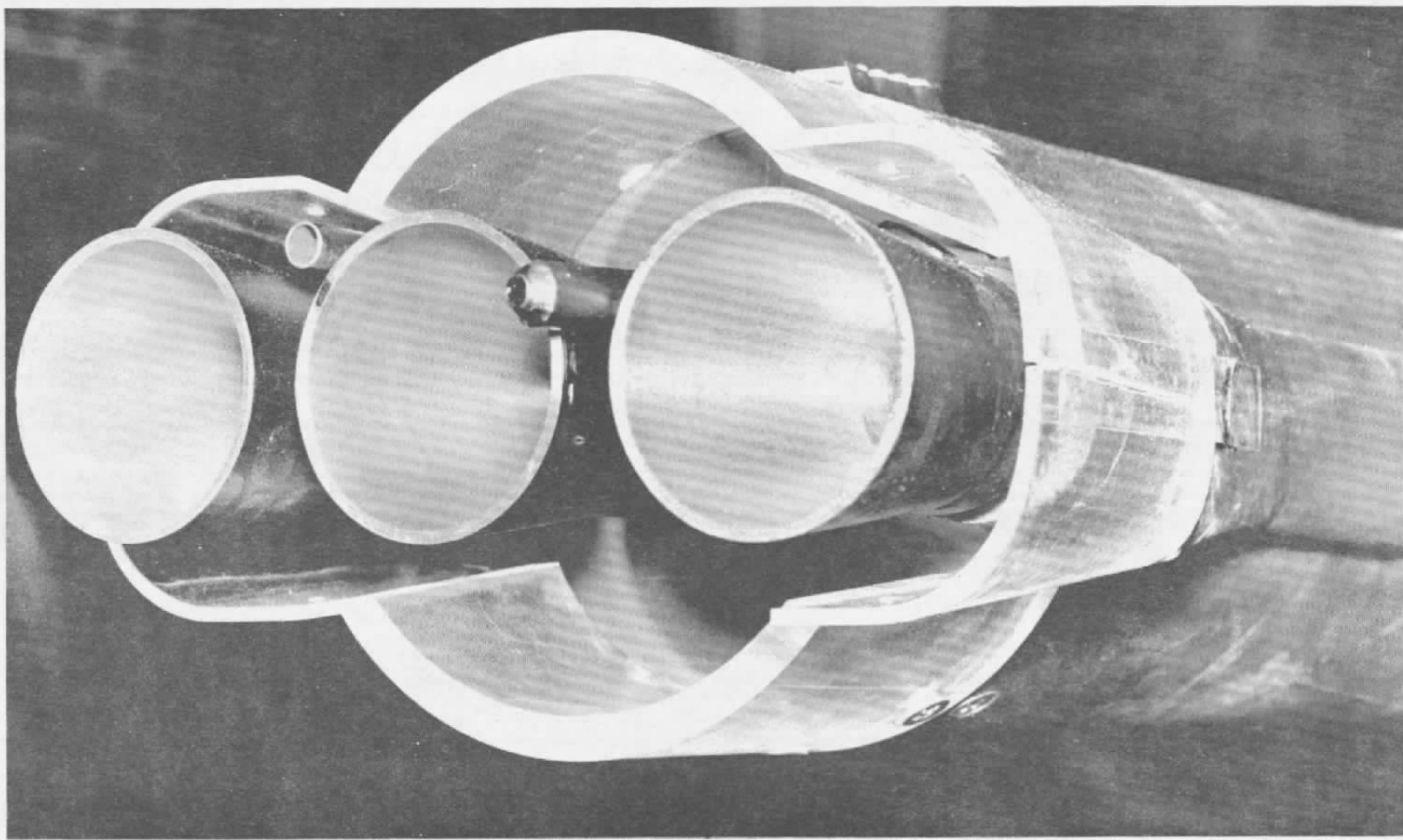
b. Booster Nozzle, $A/A^* = 5.12$, Chamber Pressure of Approximately 150 psia

Fig. 8. Schlieren Photographs of Model Nozzles



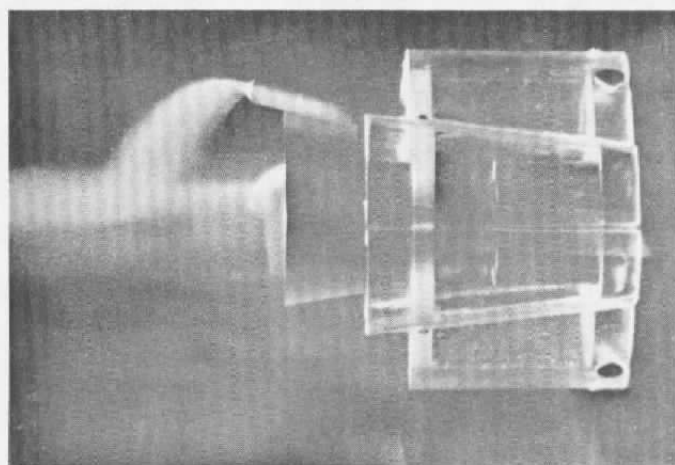
a. Top View

Fig. 9 A Test Configuration of a Cold Flow Atlas Model



b. End View

Fig. 9. Concluded



**Fig. 10 Smoke Tests with a Special Test Configuration
of a Cold Flow Atlas Model without External
Flow (smoke velocity is approximately Mach 0.50;
note booster turbine exhaust canted overboard
and straight sustainer turbine exhaust duct.)**

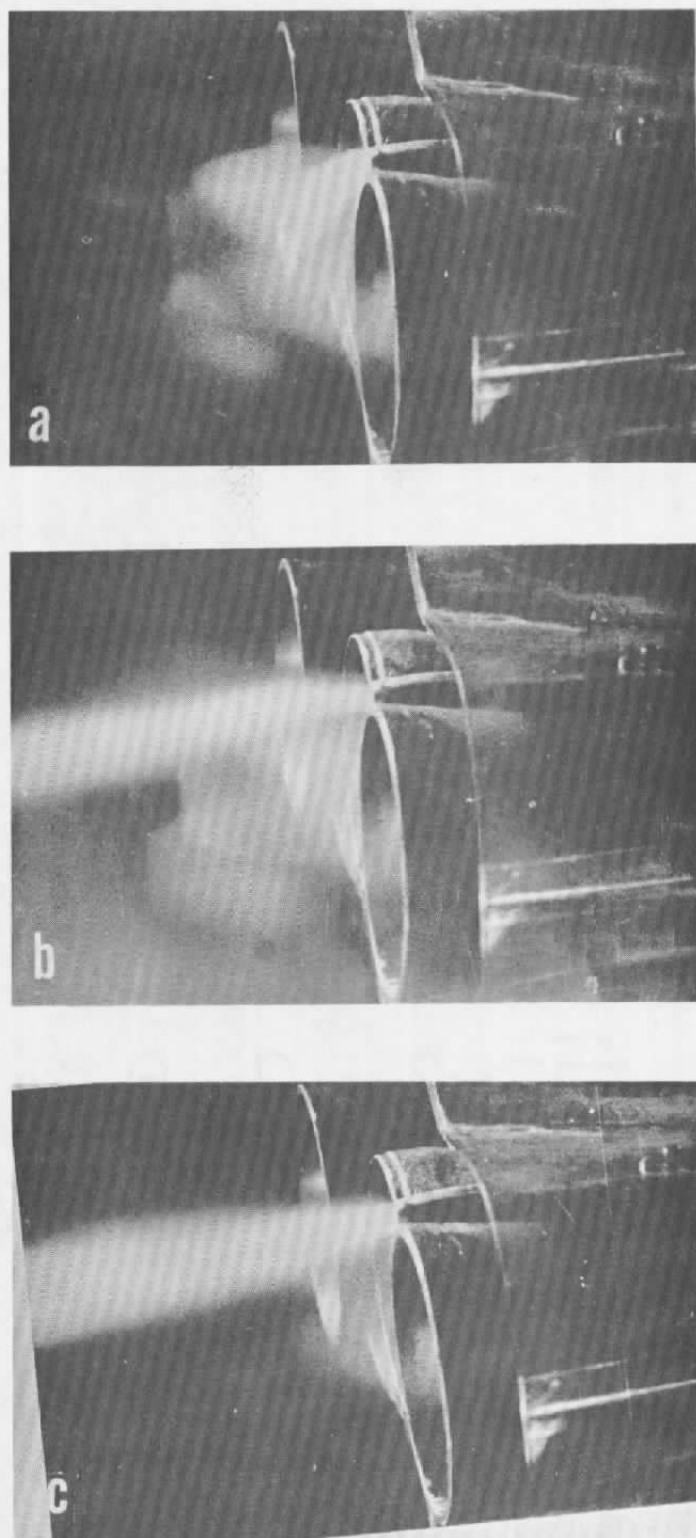


Fig. 11 Effect of an Increase in Velocity of Turbine Exhaust Gases (Special Test Configuration)

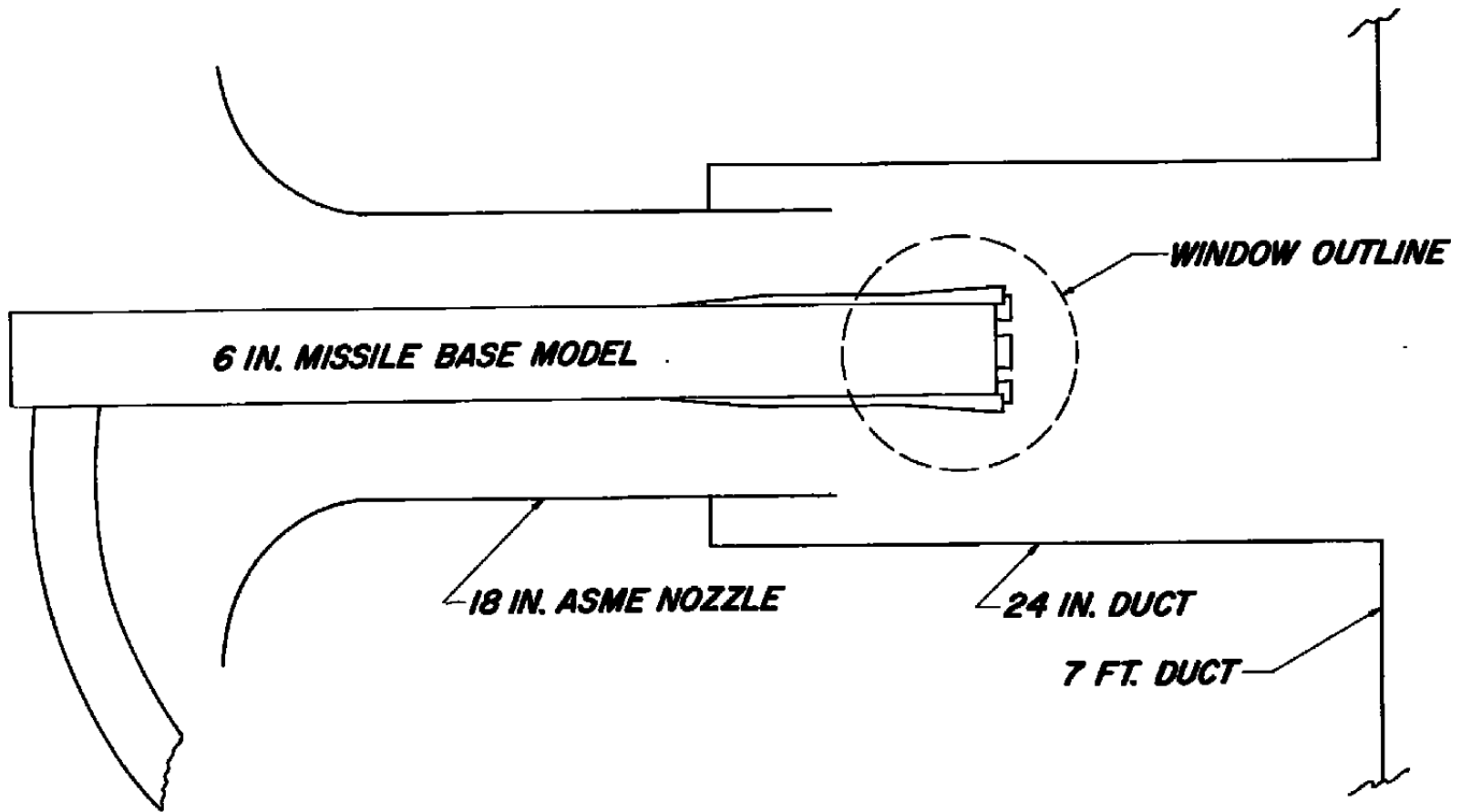
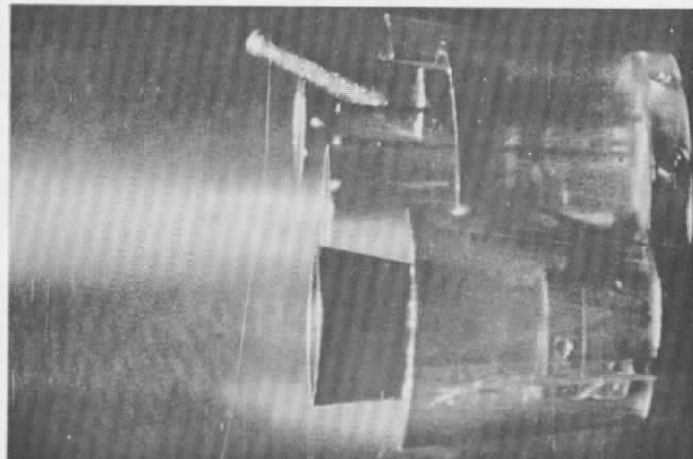
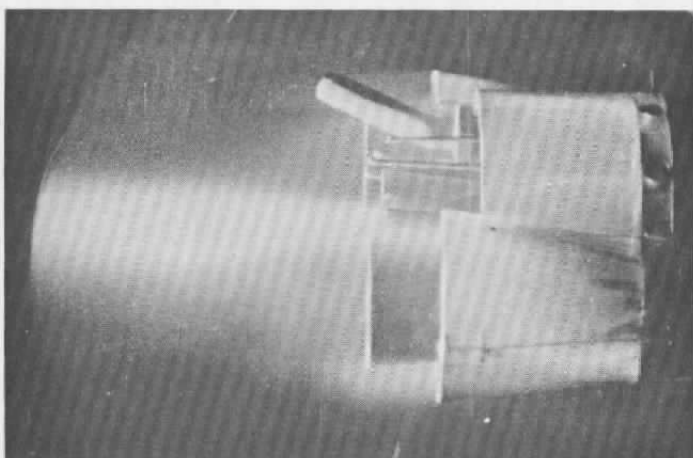


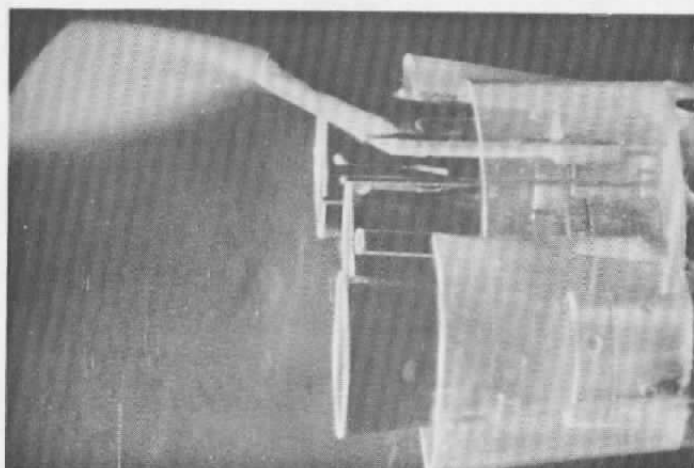
Fig. 12. Subsonic Test Chamber



a. External Flow Velocity Mach 0.33; Smoke Velocity
Mach 1.3



b. External Flow Velocity Mach 0.80; Mica Velocity
Approximately Mach 1.3



c. External Flow Velocity Mach 0.80; Mica Velocity
Approximately 0.60

Fig. 13 Tests of an Atlas Cold Flow Model (Special Test Configuration) in a Subsonic Test Chamber

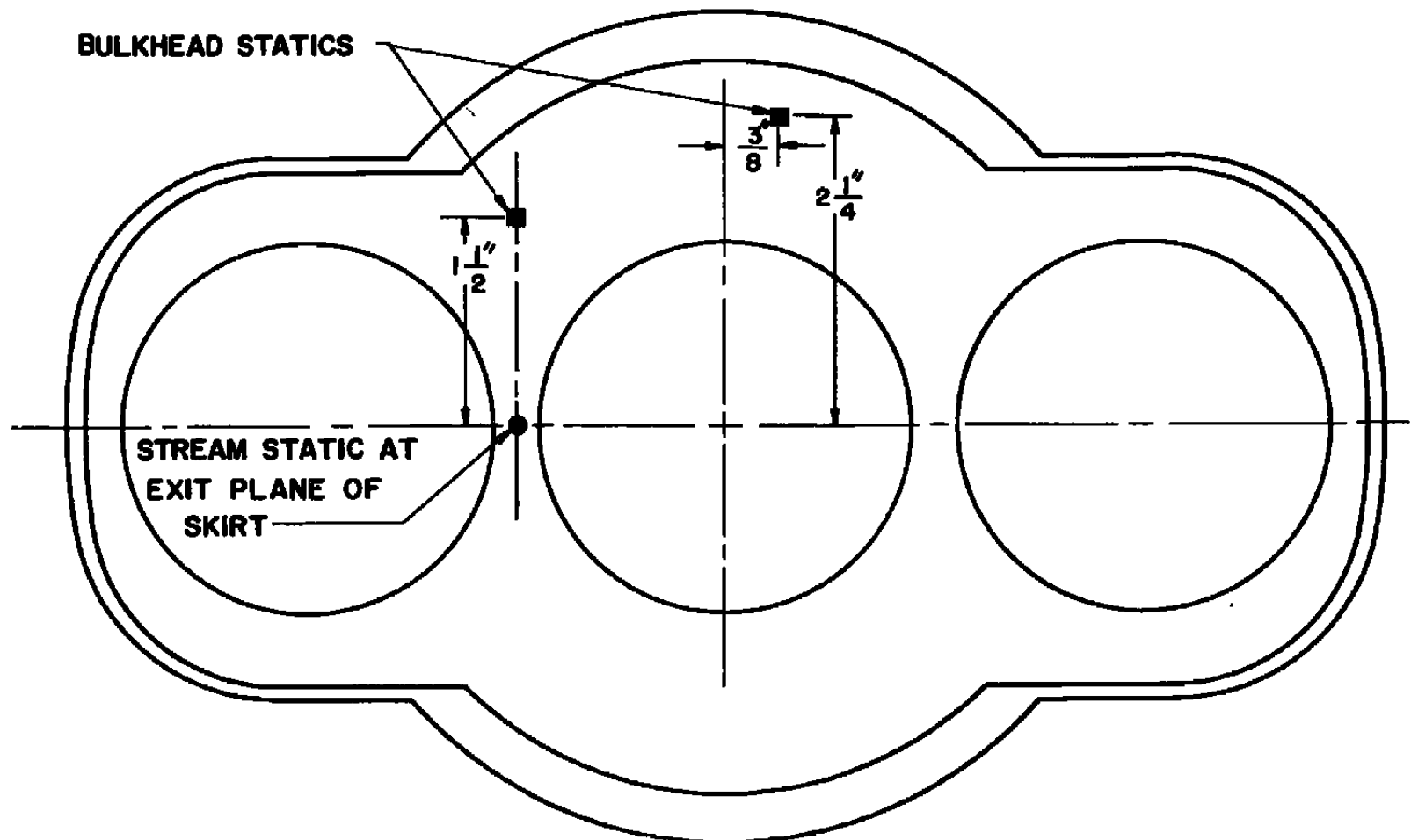


Fig. 14. Location of Base Pressure Instrumentation

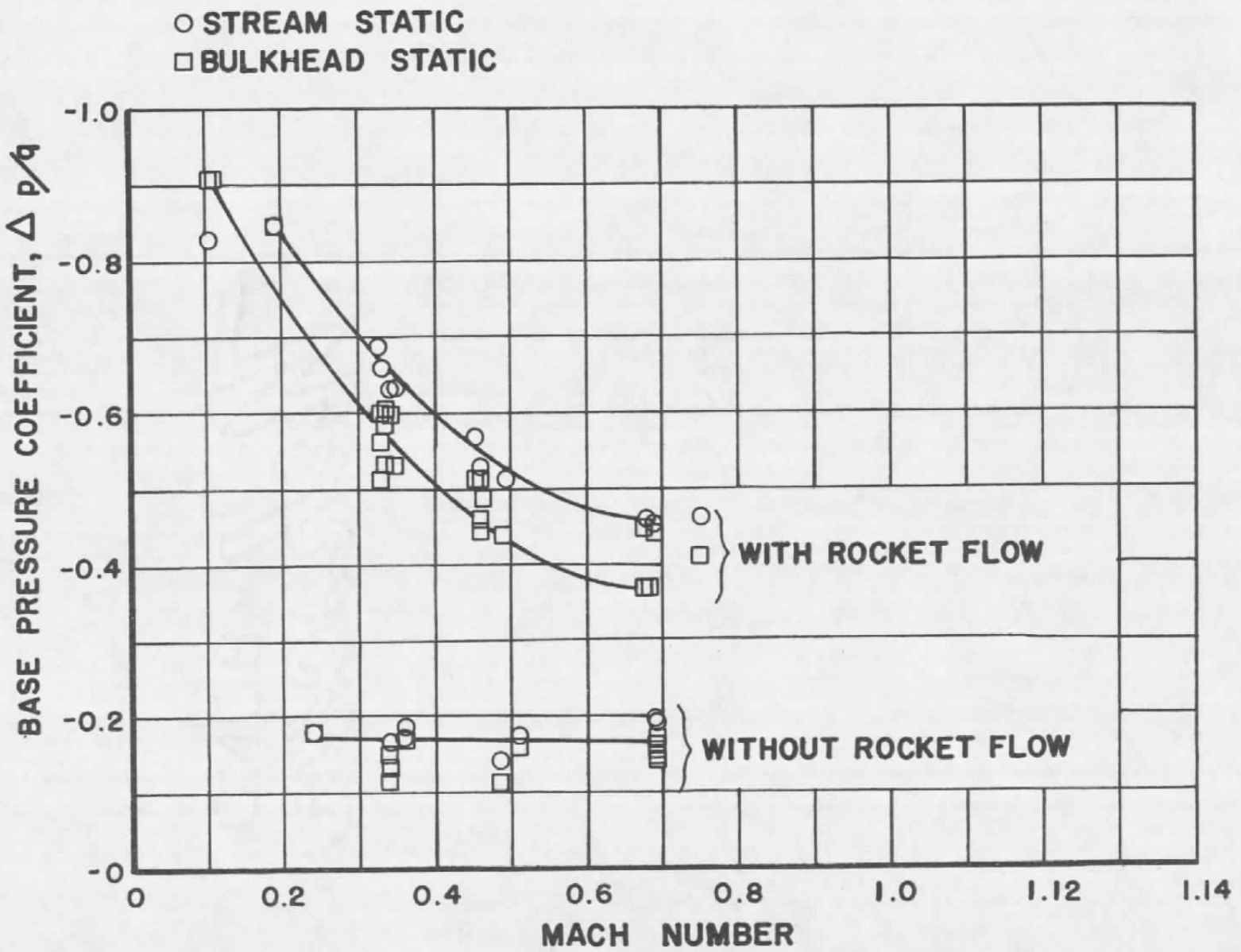


Fig. 15. Base Pressure Coefficients for the Atlas Cold Flow Model as a Function of the External Flow Velocity

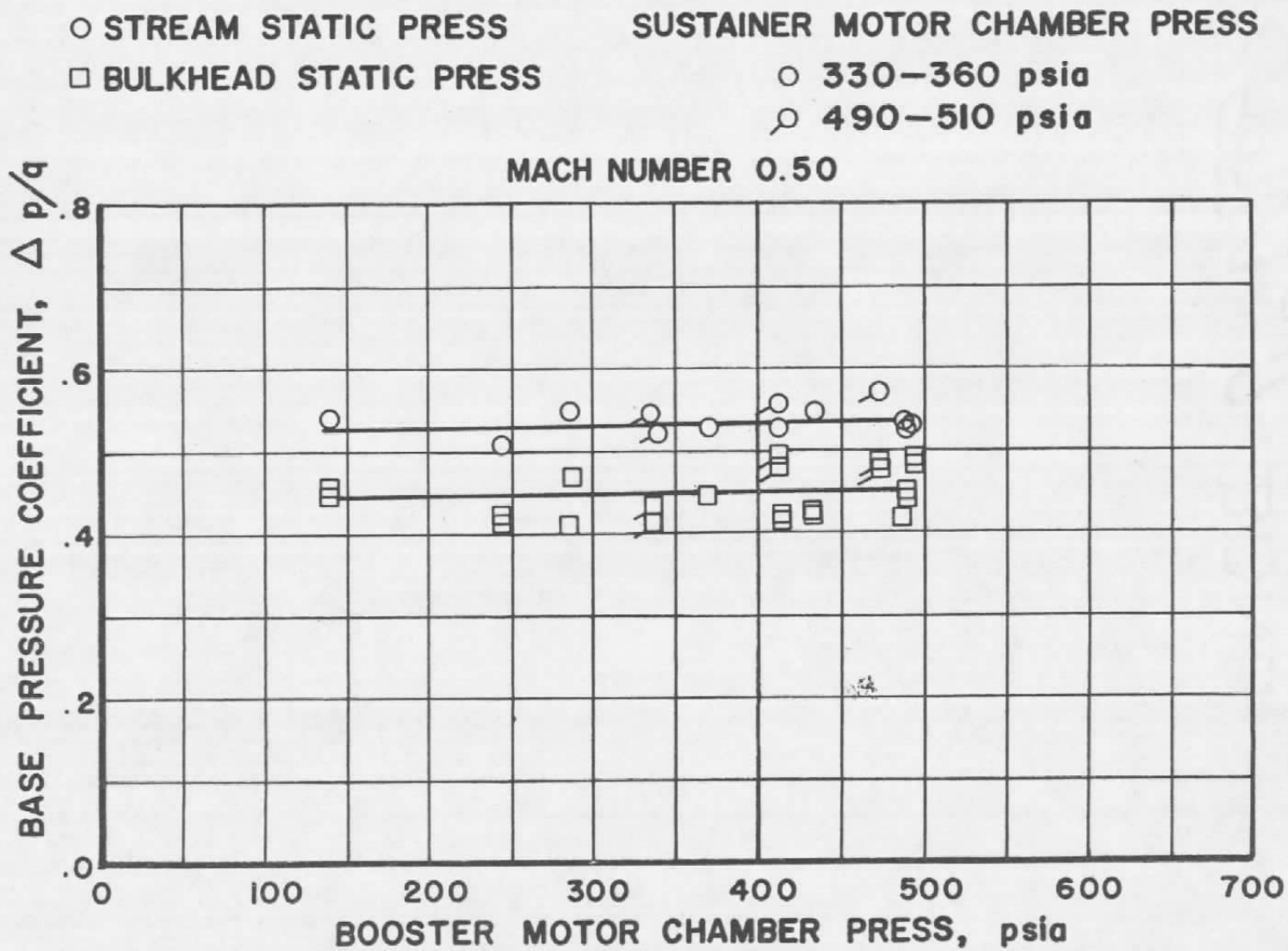


Fig. 16. Influence of Rocket Motor Chamber Pressure on the Base Pressure Coefficient

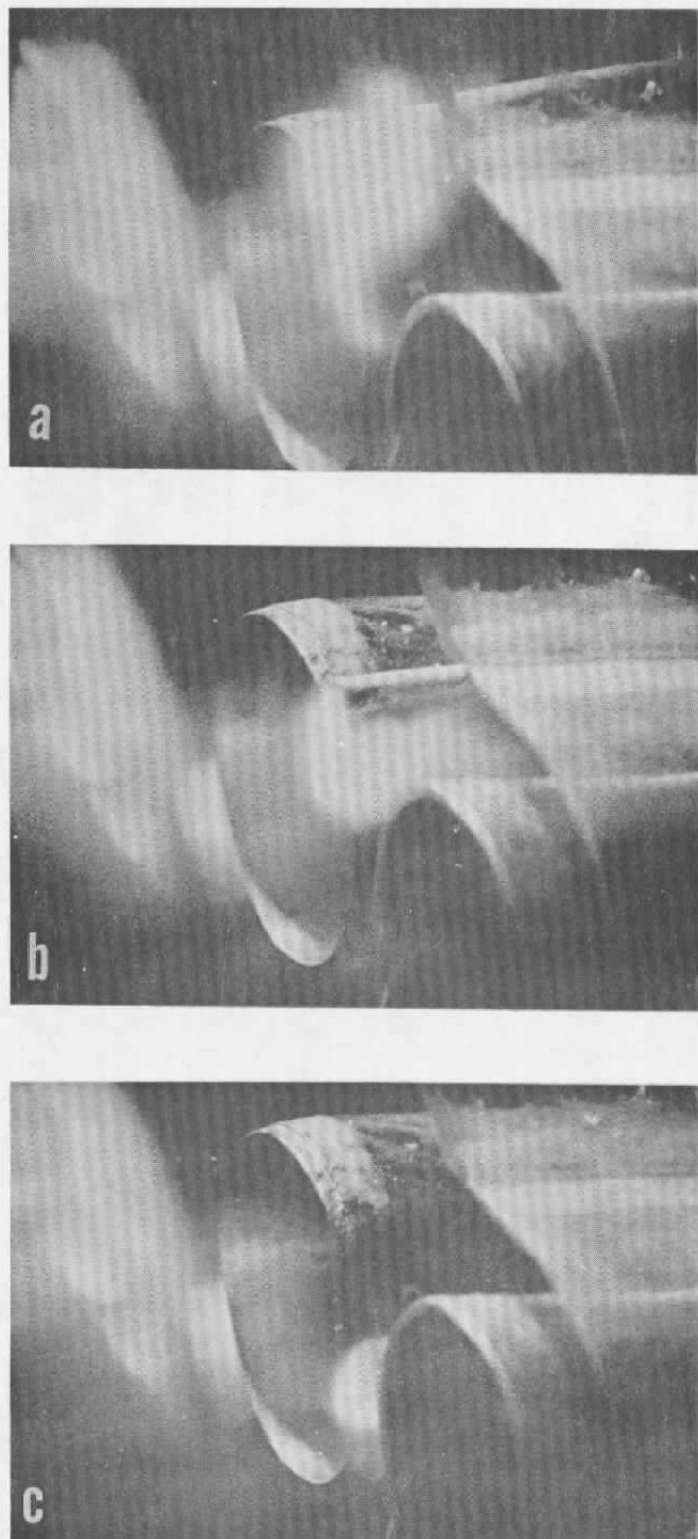
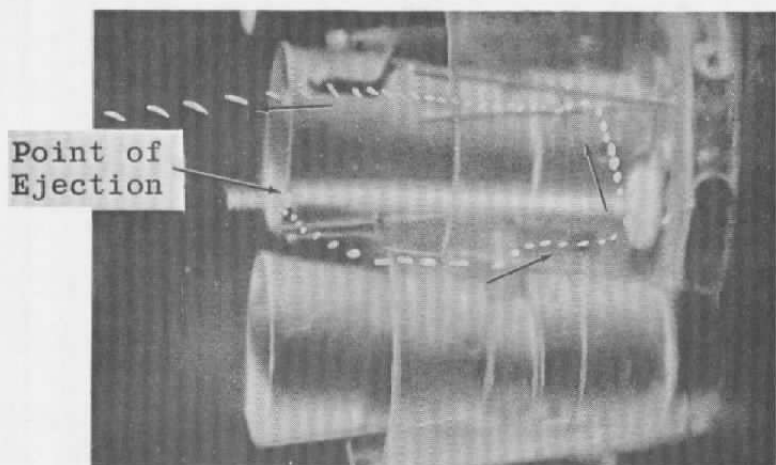
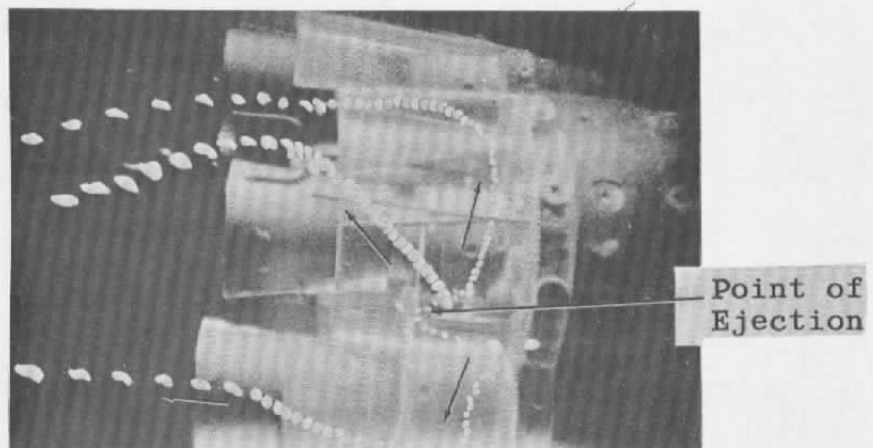


Fig. 17. Smoke Studies Using a Probe Which Could Be Rotated around Periphery of Sustainer Nozzles



a. Path of 1/16-in. Plastic Bead Ejected into Base of Atlas Cold Flow Model



b. Paths of Several Styrofoam Particles Ejected into Base of Atlas Cold Flow Model

Fig. 18. Studies of Base Flow Patterns Using Small Particles

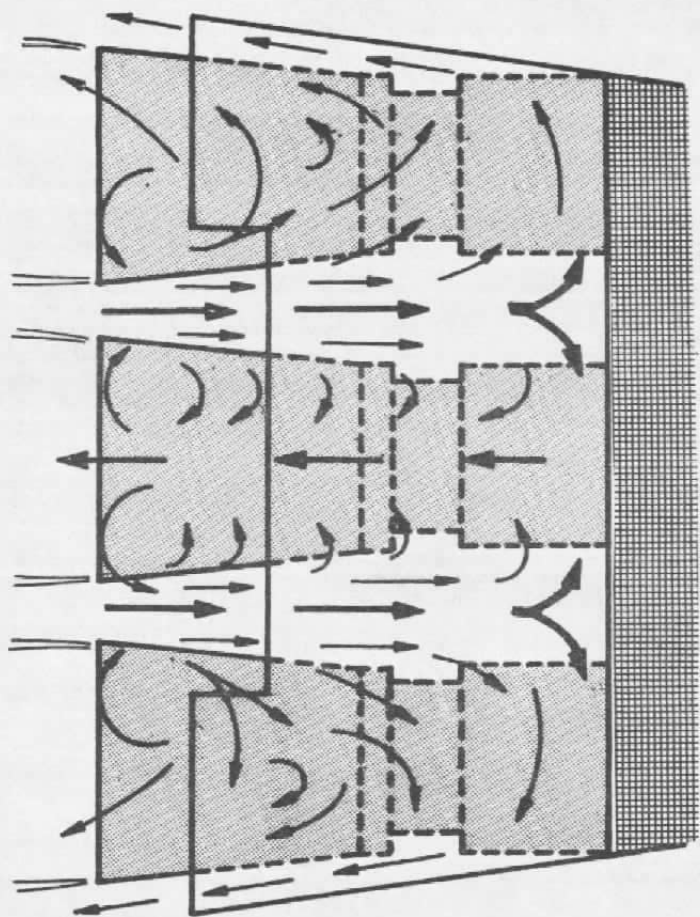
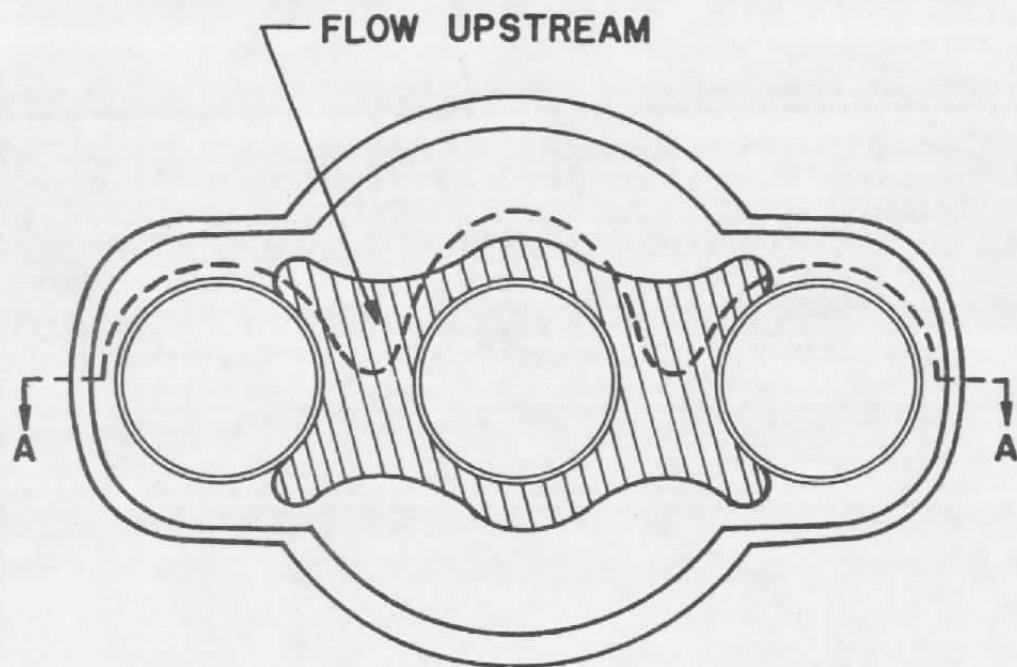


Fig. 19. Flow Pattern in Base of Atlas Cold Flow Model Based on Tests Using Small Particle Ejection Method

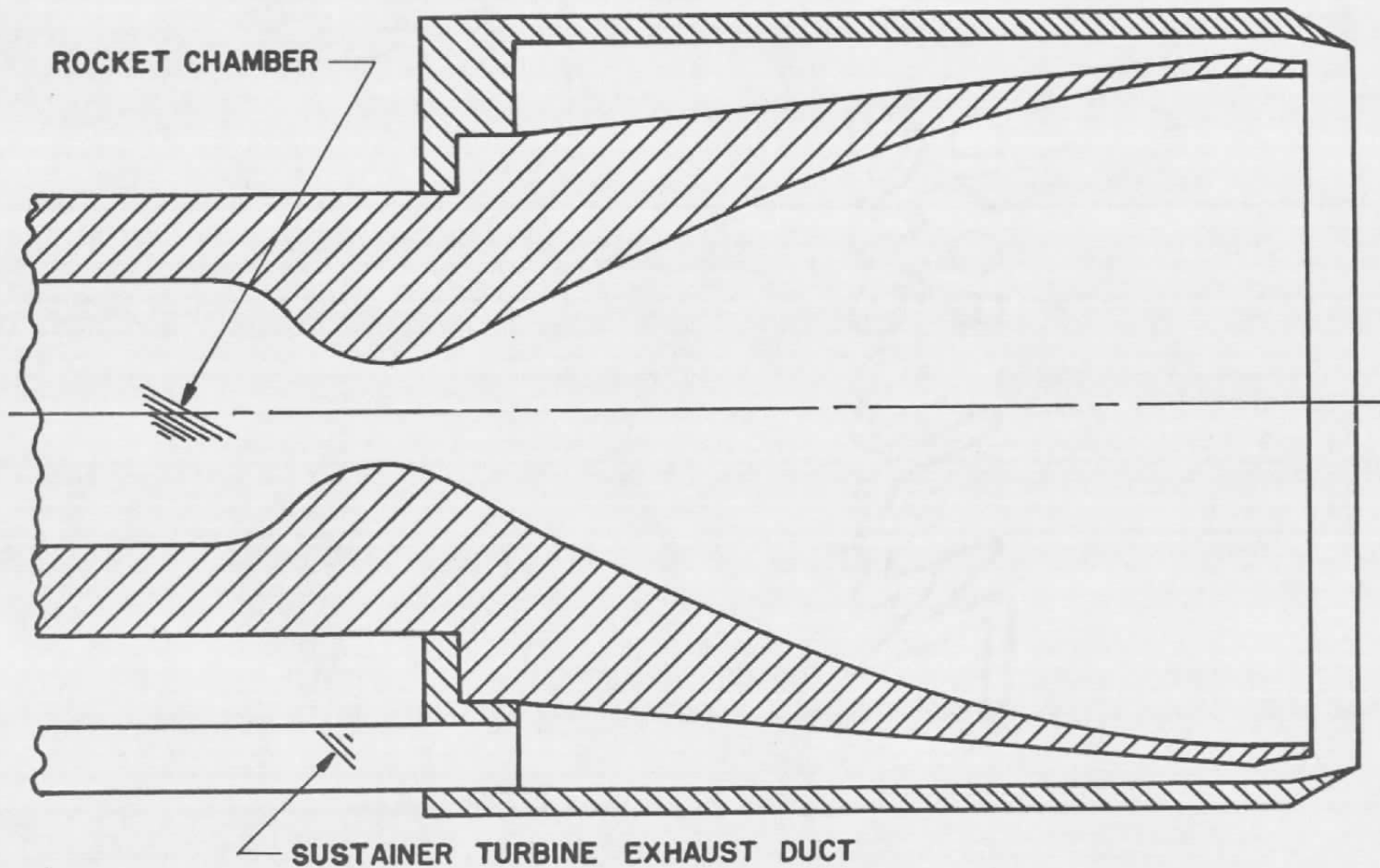
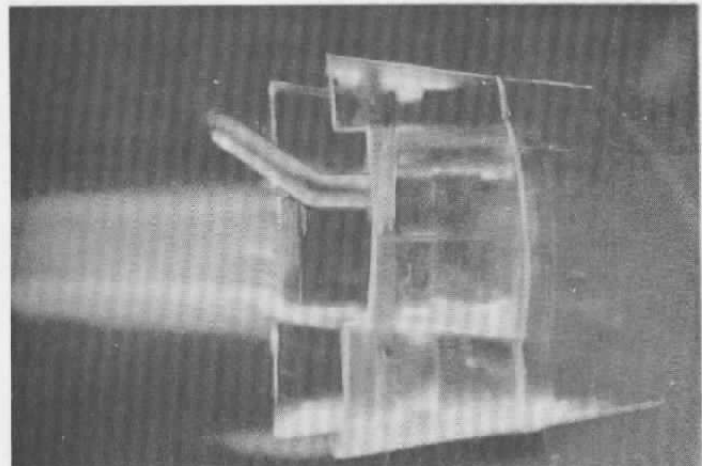
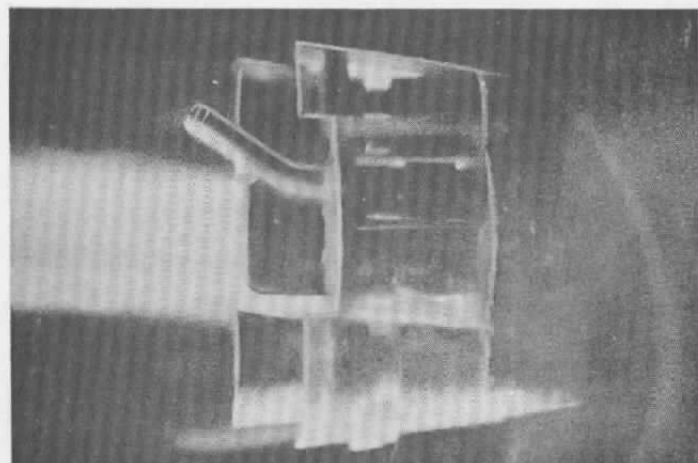


Fig. 20 Cross Section of Annular Sustainer Turbine Exhaust Duct and Sustainer Motor Model Nozzle
(Similar to NAA-Rocketdyne Exhausterator Design)



Exhaust Pressure
of 20 psia



Exhaust Pressure
of 51 psia

Fig. 21 Tests with an Annular Sustainer Turbine Exhaust Duct at External Flow Velocity of Mach 0.50 (Similar to NAA-Rocketdyne Exhausterator Design)



DEPARTMENT OF THE AIR FORCE
HEADQUARTERS ARNOLD ENGINEERING DEVELOPMENT COMPLEX (AFMC)
ARNOLD AIR FORCE BASE TENNESSEE

14 Sept 2014

MEMORANDUM FOR: DTIC

FROM: AEDC/XP2 (STINFO Officer)

SUBJECT: Change in Distribution Statement

1. DTIC currently holds AEDC report (AEDC-TR-58-12 titled *(U) Some Studies of the Flow Pattern at the Base of Missiles with Rocket Exhaust Jets* and assigned DTIC accession number AD0239465) that has been reviewed and determined to be public releasable (assigned AEDC public release number AEDC2014-185). We respectfully request that your organization update the distribution statement from the present Distribution Statement C to "Distribution Statement A – Approved for public release; distribution is unlimited", effective the date of this memorandum.
2. If you have any questions, comments or need further information, you can reach me at 931-454-7221 or by email at james.stewart.58@us.af.mil.



JAMES R. STEWART
STINFO OFFICER
AEDC/XP2